Neutron diffraction residual stress measurements in suspension HVOF sprayed Al2O3 and YSZ coatings.

OWOSENI, T., BAI, M., HUSSAIN, T., FAISAL, N.H., LEE, T.L., KELLEHER, J.

2019

ITSC 2018—Proceedings of the International Thermal Spray Conference
May 7-10, 2018, Orlando, Florida, USA
F. Azarmi, K. Balani, T. Eden, T. Hussain, Y.-C. Lau, H. Li, K. Shinoda, editors

Neutron Diffraction Residual Stress Measurements in Suspension HVOF Sprayed Al_2O_3 and YSZ Coatings

T. Owoseni, M. Bai, T. Hussain
Faculty of Engineering, University of Nottingham, Nottingham, NG7 2RD, UK

N. H. Faisal
School of Engineering, Robert Gordon University, Aberdeen, AB10 7GJ, Scotland, UK

T. L. Lee, J. Kelleher
ISIS Neutron Source, Rutherford Appleton Laboratory, Harwell Oxford Didcot OX11 0QX, UK

Abstract

Thermally sprayed coatings have residual stresses due to the processing techniques where the particles go through thermal softening / melting, high velocity impact and rapid solidification. The nature and magnitude of residual stresses in these coatings determine the bond strength and failure mechanisms. This investigation thus involves a non-destructive neutron diffraction residual stress evaluation of suspension high-velocity oxy-fuel (S-HVOF) thermal sprayed alumina and YSZ coatings onto 304 stainless steel substrates. SHVOF spray is a high deposition efficiency process to deposit coatings from sub-micron or nanometric feedstock particles. Neutron diffraction measurements were performed at the UK ISIS facility, using ENGIN-X pulsed neutron diffractometer to obtain through thickness residual stress profiles. The Z-scanning method was used to avoid pseudo-strains in the neutron diffraction measurements near the coating surface whereby the incident neutron beam/gauge volume was partially submerged and traversed vertically out of the horizontal coating surface. The residual stress in the alumina coating was compressive across the whole thickness while the stress changed from tensile to compressive in the YSZ coatings. The residual stress measurements were complemented by lab based X-ray diffraction residual stress measurement techniques. Depth sensing indention of the coatings were also performed to gain a comprehensive understanding of the stresses in SHVOF sprayed ceramic coatings.

Keywords: Neutron diffraction, X-ray diffraction, Residual stress, S-HVOF, Thermal spray coating, Alumina, YSZ

Introduction

One of the surface engineering techniques that has been used and being studied for improved surface modification is thermal spray. Thermal spray is a widely used technique for ceramic materials for high value engineering applications, for example thermal spray has been used to deposit Al_2O_3 (in electrical insulation, corrosion and wear applications) and YSZ (in thermal barrier coatings and solid oxide fuel cell (SOFC)) [1]. Stresses however are generated in coatings due to this processing technique. The overall performance and lifetime of these coatings are subject to the magnitude and nature of the residual stresses in the coatings [2]. Residual stress is the inherent stress in a material keeping it at equilibrium when load is applied to it.

Depositing nanostructured coatings is considered to offer engineered surface with improved performance [3]. Suspension high velocity oxy-fuel (SHVOF) is an emerging spray technique capable of depositing sub-micron to nanometric size feedstock [4,5]. It has been demonstrated that reduced feedstock particle sizes would increase the residual stress in thermal spray coatings [6]. The increase in stress has been attributed to reduced interparticle spacing that makes the coating build up materials closely packed. Residual stress measurement techniques vary in their accessibility and precision and they include neutron diffraction, nanoindentation, X-ray diffraction technique, synchrotron X-ray radiation, curvature method, focus ion beam milling and digital correlation neutron diffraction offered the deepest penetration measurement. These techniques have been used in the investigation of the residual stress in bulk materials and coatings [7].

Despite Al_2O_3 and YSZ being widely used and studied engineering ceramics, very limited work has been reported on the residual stress behaviour of SHVOF sprayed Al_2O_3 and YSZ coatings. A detailed understanding of residual stress of these coatings will facilitate accelerated commercial update of these coatings. The aim of this current work is to use non-destructive technique such as X-ray diffraction and time-of-flight (TOF) neutron diffraction to investigate the residual stresses in SHVOF sprayed Al_2O_3 and YSZ coatings.

Experimental

Materials and coating fabrication

Two coatings were deposited, each from different feedstock materials. The YSZ coating was sprayed from a commercially available ethanol suspension supplied by Treibacher Industrie AG (Althofen, Austria). Based on the data sheet provided by the supplier, the suspension contains ~ 25 wt. % of ZrO_2-8 % Y_2O_3 with particle size distribution (PSD: D_{10} = 0.26 µm, D_{50} = 0.6 µm, D_{90} = 1.32 µm). The other coating was made from bespoke aqueous suspension containing ~ 21 wt. % of pure alpha Al_2O_3 powder CR1 (D_{50} = 1 µm) supplied by Baikoswki (Poisy, France). The substrates in both coatings (60 x 25 x 2 mm)

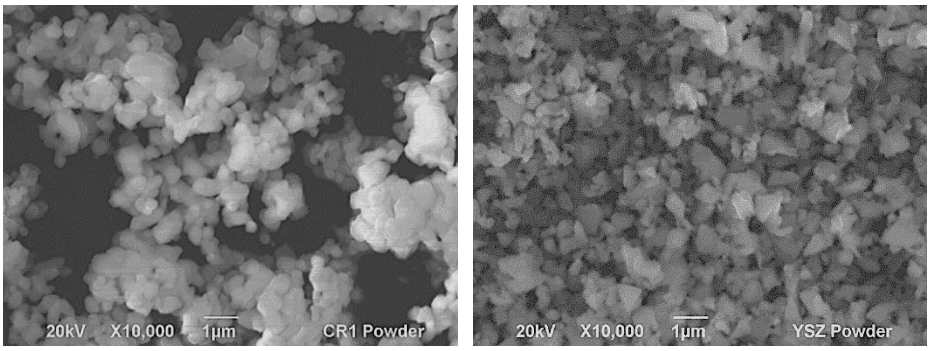

Figure 1: Secondary electron (SE) scanning electron micrograph showing (a) Al_2O_3 feedstock powder (b) YSZ feedstock powder, from dried suspension.

were AISI 304 stainless steel (SS) with nominal composition of Fe–19.0Cr–9.3Ni–0.05C (in wt. %).

Both coatings were deposited using a modified UTP TopGun HVOF spray unit from Miller Thermal Inc. (Wisconsin, USA) with axial injection of suspension directly into the combustion chamber with a 0.3 mm nozzle diameter. The suspension was delivered from a pressurized vessel maintained at 3 bar which resulted in a feed rate of 90 ml/min and 5 bar yielding 100 ml/min for the Al_2O_3 and YSZ suspensions, respectively. The complete set up was further described in [5]. The substrates were grit blasted with a blast cleaner from Guyson (Dudley, England) with fine alumina (0.125-0.149 mm) particles at 3 bar. Following grit blasting, the substrates were cleaned in industrial methylated spirit (IMS) in an ultrasonic bath for up to 10 minutes and blown dry with compressed air. The substrates were then mounted onto a rotating carousel with a vertical axis of rotation operating at 73 rpm while the spray gun traverses along the vertical axis at a speed of 5 mm/s. This resulted in a relative velocity of 1 mm/s on the substrate [8]. During spraying the samples were cooled with compressed air during deposition. Table 1 gives the detail spray parameters. The Al_2O_3 suspension was stirred for ~ 6 h at 700 rpm using overhead stirrer-IKA RW20 digital (Wilmington, USA) while the YSZ suspension was rolled for ~ 1 h with its lid in place to prevent loss of ethanol before spraying.

Table 1: SHVOF spray parameters for Al2O3 and YSZ coatings deposited onto stainless steel substrate.

Parameters	Values	
	Al_2O_3	YSZ
Fuel (hydrogen) flow rate, l/min.	612	788
Oxygen flow rate, l/min.	306	337
Flame power, kW	101	110
Suspension flow rate, ml/min.	90	100
Spray distance, mm	85	85
Number of passes	41	26
Spray gun traverse speed, mm/s	5	5

Characterization

200 ml of each suspension was heated separately in a box furnace at 100 °C for 8 h to obtain dried powder and the particle size was examined with a Scanning Electron Microscopy (SEM) in secondary electron (SE) mode (see Fig. 1 (a) and (b)). The powders (as-received) and coatings (as-sprayed) were scanned on a Bruker D500 diffractometer (Siemens.AB, Germany) with a Cu Kα radiation source (1.54 Å) and a point detector for phase identification. Powders were scanned with $10° - 120° 2\theta$, step of 0.05° and dwell of 4s for phase analysis. Each of the coatings were scanned for phase analysis and residual stress analysis. Both coatings in their as-sprayed form where scanned with $10° - 80° 2\theta$, step of 0.025° at a dwell of 4s for phase analysis. XRD scanned data were analyzed using diffracsuite EVA (Bruker Software). The residual stress scan was however completed on the D8-Discover (Bruker AXS Inc., Madison, WI, USA) with Cu Kα radiation source (1.54 Å) the parameters are as stated in Table 2. The scanned data was then analysed using Stress 2.0 (PANalytical, Almelo, The Netherlands).

Table 2: Residual stress scan parameters.

Parameters	Coatings	
	Al_2O_3	YSZ
2θ, °	139-152	111-120.6
Step size, °	0.1	0.1
Dwell time, sec./step	8	8
orientation angle, φ°	0, 45, 90	0, 45, 90
Tilt angle, ψ°	0-60	0-60
PDF card	$\gamma - Al_2O_3$,10-0425	Tetragonal, 01-070-4431
Peak	145.3°	116.2°

The microstructure of the coatings were obtained from carbon coated top surface and cross-sections using JEOL 6490 from JEOL Ltd. (Tokyo, Japan). Transverse sections in 12 x 25 x 2 mm sizes were obtained from table top precision cutter using

SiC disc. The samples were hot mounted in conducting resins (Bakelite) and then mirror polished to 1 µm. Secondary electron (SE) images of the top surface morphology were obtained at 20 kV acceleration voltage with a spot size of 50 (au) at a working distance of 10 mm. The cross-section images were taken in the backscattered electron (BSE) compo mode with the same parameters.

Elastic modulus of the coatings were calculated from the results of the depth-sensing indentation (DSI) performed on the polished cross section of the coatings mounted in conducting resins to eliminate the chance of compound elasticity data. The DSI was carried out at room temperature on the Platform 3 rig produced by Micro Materials Ltd (Wrexham, UK) using a Berkovich indenter tip. The loading-dwell-unloading scheme was used maintaining a peak load of 20 mN for 2 s and a rate of 4 mN/s during loading and unloading stages for a total of 25 indentations per sample in five rows adequately spaced from coating surface and coating/substrate interface. The elastic modulus was then estimated by Oliver and Pharr method [9] where the reduced modulus of the indenter system (E_r), the modulus of the indenter material (E_i) and the coating modulus (E_c) are related as in equation (1).

$$\frac{1}{E_r} = \frac{1-v_c^2}{E_c} + \frac{1-v_i^2}{E_i} \qquad \text{Equation 1}$$

In equation (1), v is poisson ratio with c and i representing coating and indenter repectively. The E_i and v_i are taken as 1140 GPa and 0.07 respectively [10]. The Poisson ratio of bulk alumina (0.22) and YSZ (0.31) [11] were used for the coatings in each case.

Neutron diffraction residual strain measurements were completed on the two coatings at the UK's Science and Technology Facilities Council (STFC) using the time-of-flight (TOF) neutron strain scanner (ENGIN-X) at the ISIS facility. Detailed set-up of the neutron diffractometer is published elsewhere [12]. The incident neutron beam/gauge volume was partially submerged and traversed vertically through the coating thickness. The gauge volume was obtained as 4 mm x 4mm x 200 µm with double slits positioned along the neutron incident path. The effective sample/slit separation was ~ 135 mm for the Al_2O_3 coating and ~ 155 mm for the YSZ coating. Pulverized coating samples were scanned for the strain-free state as reference. The residual strain in the coatings was estimated using the single peak approach [13] whereby the shift in the individual γ-Al_2O_3 peak, tetragonal-YSZ and Fe (α) were realated to lattice spacing of the strain-free sample as in equation (2).

$$\varepsilon_c = \frac{d_{c-d_o}}{d_0} \qquad \text{Equation 2}$$

In equation 2, ε is the strain, d is lattice spacing while c signifies coating and d_0 is the lattice spacing from stress-free samples. The elastic stress was then calculated from the obtained strain values and the elastic modulus assuming plane stress condition.

Results and discussion

The scanning electron micrographs of the coatings shown in Fig. 2 present the top surface morphology and the cross sectional views. The Al_2O_3 coating consists of adequately molten splats covering the entire substrates top face as shown in Fig. 2 (a).

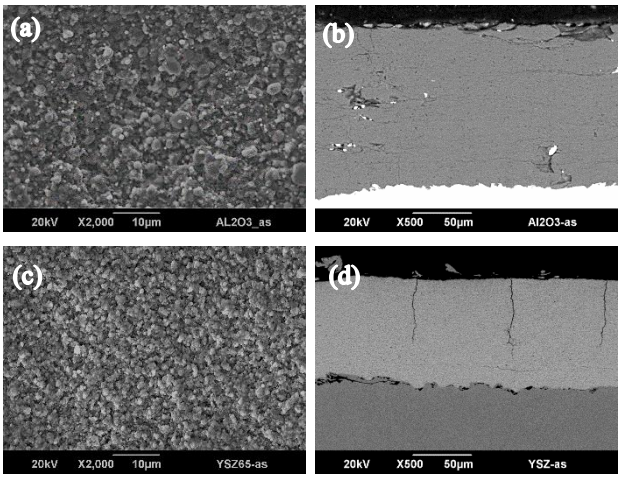

Figure 2: SEM micrographs of SHVOF coatings showing (a) top surface molten splats of Al_2O_3 coating (b) through thickness of BSE cross-section of Al_2O_3 coating (c) top surface molten splats of YSZ coating (d) through thickness of BSE cross-section of YSZ coating

The thickness of the coating is ~ 200 ± 2 µm as shown in Fig. 2 (b).The cross section also shows horizontal cracks and voids at the inter-spray layers. The coating-substrate interface shows good bonding suggesting good flow of molten splats that allows sufficient mechanical interlocking on the grit blasted substrate [14]. The YSZ coating appears not to attain similar degree of feedstock melting, looking at the top surface morphology presented in Fig. 2 (c). Its cross sectional view presented in Fig. 2 (d) shows the coating thickness is ~ 120 ± 1 µm and also suggests the feedstock may not have melted sufficiently to ensure intimate flow into the roughened surface of the substrate. This is further supported by the obvious voids at the coating-substrate interface even though there is no clear case of debonding. The observed difference in feedstock melting condition is connected with the thermal properties of the feedstock materials. This has engendered different deposition flame power The cross section of the YSZ coating also shows vertical cracks which has been reported for ethanol based YSZ suspension feedstock deposited by SHVOF [5,15,16].

The XRD patterns of both coatings presented in Fig. 3 show the identified phases in the as-received feedstock and the as-sprayed coatings. The Al_2O_3 feedstock shows pure alpha phase which has then transformed to a mixture of amorphous and gamma Al_2O_3 in the deposited coating with sparse amount of retained feedstock as shown in Fig. 3 (a). This is consistent with observed microstructure in thermally sprayed alumina coatings [8,17]. The YSZ feedstock on the other hand contains both monoclinic and tetragonal phases. Upon deposition, the entire

monoclinic phase got transformed to the much desired tetragonal phase as shown in Fig. 3 (b). The complete transformation therefore shows the feedstock particles received sufficient heat transfer and could only have solidified in-flight to produce the surface condition presented earlier on. This assertion agrees with the report of Bai et al. [5] where the surface roughness of YSZ coating sprayed from ethanol based suspension was observed to be higher compared to its aqueous based counterpart. The observation was attributed to the rather solidified finer particles reaching the substrate.

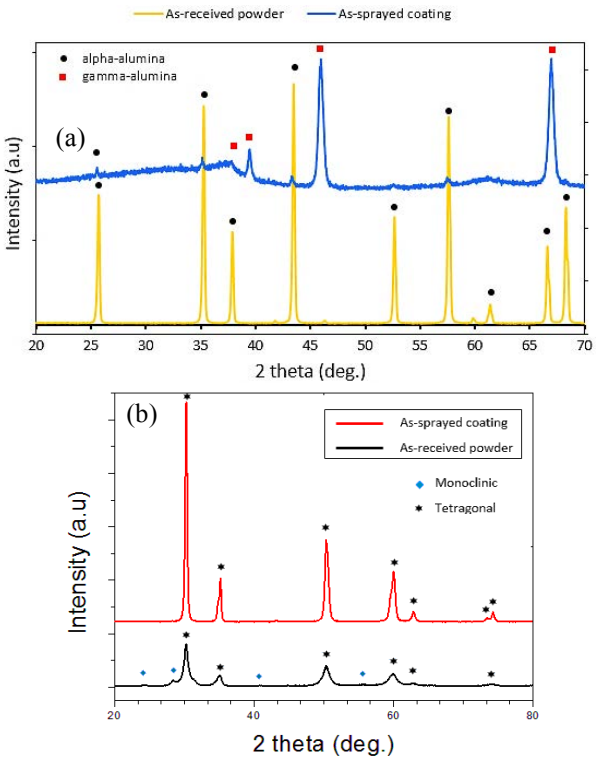

Figure 3: X-ray diffraction profile showing (a) Al_2O_3 as-received feedstock and as-sprayed coating (b) YSZ as-received feedstock and as-sprayed coating

Neutron diffraction patterns of the through thickness scan of the two coatings are shown in Fig. 4. The Al_2O_3 coating again shows the presence of gamma-Al_2O_3 (Fig. 4 (a)) in congruence with the XRD pattern of the coating and the specific peaks used in the residual strain estimation are identified as gamma (440) and gamma (400). This has also been reported by Ahmed et al. [18] where the residual strain of APS and HVOF deposited Al_2O_3 coatings were investigated. The tetragonal phase also shows as the only phase in the pattern of the YSZ coating shown in Fig. 4 (b). The strong Fe (α) peak shown in the pattern could have been from the incident neutron beam scanning the coating and substrate simultaneously despite the double slit inserted along the incident path to minimize divergence and ensure a concise gauge volume [12].

The residual strain trend observed for the identified peaks in the Al_2O_3 coating was similar; as such the average values are presented in Fig. 5 (a). The strain was entirely compressive in the coating with a value of – 520, 0.1 mm from the coating

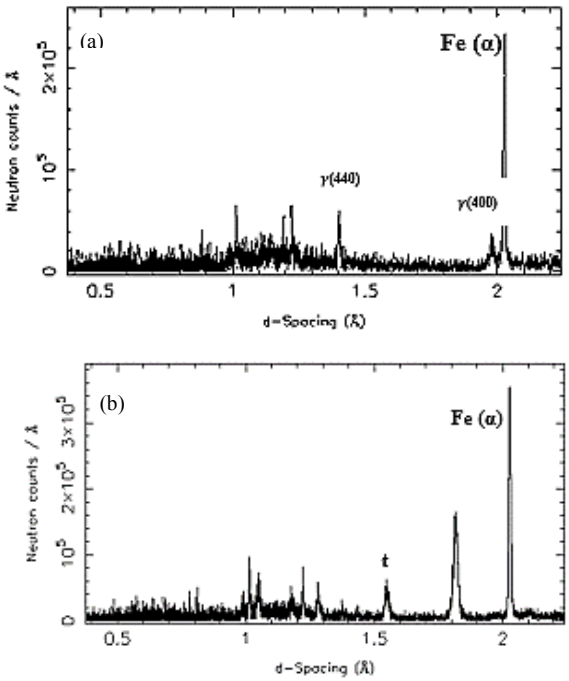

Figure 4: Neutron diffraction pattern showing peaks identified and used for residual strain estimation (a) Al_2O_3 coating (b)YSZ coating

surface, and a peak value of – 1395 at the coating substrate interface. It was however tensile-compressive transition in the substrate. The residual strain in the YSZ coating transit from tensile to compressive in the coating and entirely tensile in the substrate, as shown in Fig. 5 (b). The maximum strain (- 1481) is at the coating/substrate interface while its value near the coating's surface was 527.

The corresponding neutron diffraction residual stress (ND-RS) in the coatings is presented in Fig. 6 (a) and (b).
The stress profile in both coatings show similar trend of compressive towards the substrate with a counter balance tensile stress away from the substrate. This might explain why the two coatings did not show any sign of debonding at the coating substrate interface. The average XRD residual stress (XRD-RS) of the coatings was estimated using a differential technique that eliminates the need for a reference strain/stress free sample. A linear relationship is evoked between the surface stress in any direction and the measured interplanar lattice spacing according to Equation (3) [19]. This is called the $sin^2\psi$ technique.

$$\sigma_\phi = \left(\frac{E}{1+\nu}\right)\frac{1}{d_{(\phi\psi)0}}\left(\frac{\Delta d_{\phi\psi}}{\Delta sin^2\psi}\right) \qquad \text{Equation 3}$$

Where $d_{(\phi\psi)0}$ and $\left(\frac{\Delta d_{\phi\psi}}{\Delta sin^2\psi}\right)$ are the intercept and slope of the plot of $d_{(\phi\psi)}$ against $sin^2\psi$, as shown in Fig. 7 (a) and (b) for the Al_2O_3 and YSZ coatings, respectively. E and ν have their usual meanings.

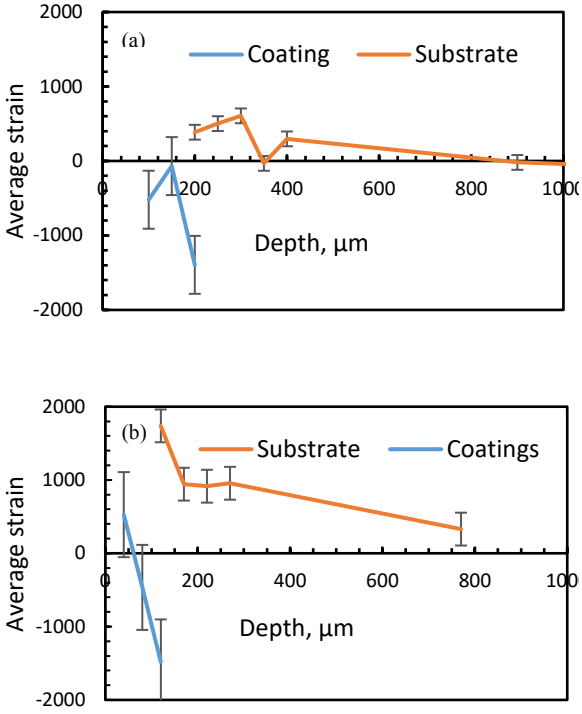

Figure 5: neutron diffraction residual strain profile (a) Al_2O_3 coating (b) YSZ coating

The values of the elastic modulus of the coatings measured by depth sensing indentation technique are 160 ± 6 GPa for the Al_2O_3 coating and 142 ± 13 GPa for the YSZ coating. X-ray does not penetrate more than 6 µm in coatings [20].

The obtained values XRD-RS can only be compared to the near surface values of the ND-RS owing that essentially, the XRD-RS is – 20.1 MPa and the ND-RS is – 19.7 MPa for the Al_2O_3 coating. These values are quite low compared to reported values for APS and HVOF sprayed Al_2O_3 coatings whose average in-plane stress was stated as 220 MPa and 136.5 MPa, respectively [21]. Similarly, the XRD-RS and the ND-RS in the YSZ coating are of the same order of magnitude each one yielding 57.7 MPa and 61.1 MPa, respectively. It should be noted that in both coatings the order of magnitude and nature of the stress are preserved.

Conclusions

For the first time, residual stress of SHVOF sprayed Al_2O_3 and YSZ coating has been investigated using combination of the time-of-flight (TOF) neutron diffraction and X-ray diffraction techniques. It has been equally demonstrated that SHVOF is able to deposit coatings of up to ~ 200 µm with reasonable integrity. That is sufficient for a TOF neutron diffraction residual stress experiment. In regard to the techniques used for the residual stress measurement, the following conclusions can be drawn:

- The surface residual stress in SHVOF sprayed A_{l2O3} and YSZ coatings are of the same order of magnitude, but A_{l2O3} has a compressive residual stress (-19.7 MPa)

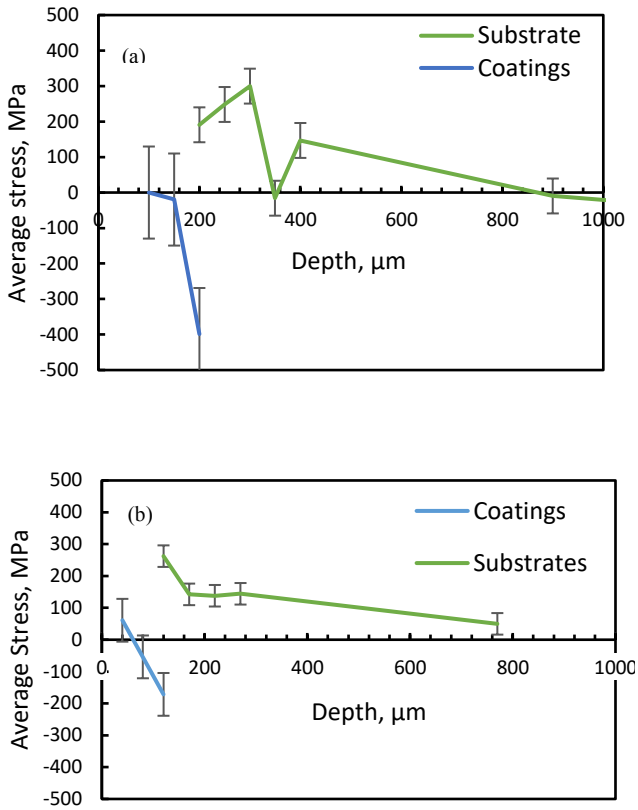

Figure 6: Neutron diffraction residual stress profile (a) Al_2O_3 coating (b) YSZ coating

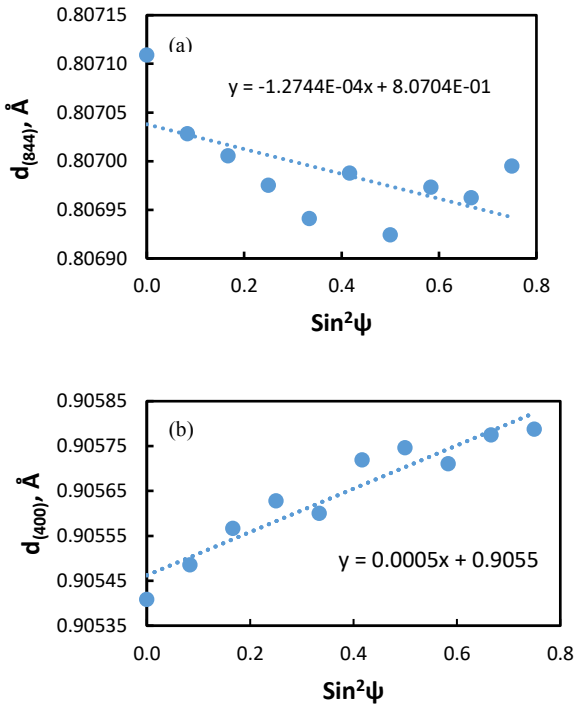

Figure 7: XRD residual stress profile (a) Al_2O_3 coating (b) YSZ coating

whereas YSZ shows a tensile residual stress (61.1 MPa) .

- Through thickness residual stress in the Al_2O_3 coating was entirely compressive but there has been tensile to compressive transition going from surface to the coating-substrate interface in the YSZ coating.
- The highest residual stress exists at the coating-substrate interface for both coatings.
- The $\sin^2\psi$ XRD residual stress results show good correleation to the resdiaul stress data measured by TOF neutron diffration technique for the coating top surface. The through thickness residual stress measurement by TOF neutron diffraction technique is an effective means of ascertaining the behaviour of SHVOF thermal sprayed coating.

Acknowledgments

The authors acknowledge beam time provided by STFC ISIS (experiment number RB1710193) for the TOF neutron diffraction experiments. T. Owoseni is supported by Petroleum Technology Development Fund (PTDF) under the overseas scholarship scheme.

References

[1] Pawlowski, L., *The science and engineering of thermal spray coatings*, John Wiley & Sons (West Sussex, 2008), pp. 28-30.

[2] Fauchais, P., Fukumoto, M., Vardelle, A., Vardelle, M., "Knowledge concerning splat formation: An invited review," *J. Therm. Spray Technol.*, Vol. 13, No. 3 (2004) pp. 337–360.

[3] Bolelli, G., Cannillo, V., Gadow, R., Killinger, A., Lusvarghi, L., Rauch, J., Romagnoli, M., "Effect of the suspension composition on the microstructural properties of high velocity suspension flame sprayed (HVSFS) Al2O3 coatings," *Surf. Coatings Technol*., Vol. 204 No. 8 (2010) pp. 1163–1179.

[4] Pala, Z., Shaw, E., Murray, J.W., Senin, N., Hussain, T., "Suspension high velocity oxy-fuel spraying of TiO2: A quantitative approach to phase composition," *J. Eur. Ceram. Soc.* Vol. 83, No. 2 (2016) pp. 801-810.

[5] Bai, M., Maher, H., Pala, Z., Hussain, H., "Microstructure and phase stability of suspension high velocity oxy-fuel sprayed yttria stabilised zirconia coatings from aqueous and ethanol based suspensions," *J. Eur. Ceram. Soc.* Vol. 38 No. 4 (2018) pp. 1878-1887.

[6] Coats, D., Krawitz, A., "Effect of particle size on thermal residual stress in WC–Co composites," *Mater. Sci. Eng. A.* Vol. 359, No. 1-2 (2003) pp. 338–342

[7] Faisal, N.H., Ahmed, R., Prathuru, A.K., Katikaneni, S.P., Goosen, M.F.A., Zhang, S.Y., "Neutron Diffraction Residual Strain Measurements of Molybdenum Carbide-Based Solid Oxide Fuel Cell Anode Layers with Metal Oxides on Hastelloy X," *Exp. Mech. Springer US ISSN* 0014-4851 (2017) pp. 1-19.

[8] Murray, J.W., Ang, A.S.M., Pala, Z., Shaw, E.C., Hussain, T., "Suspension High Velocity Oxy-Fuel (SHVOF)-Sprayed Alumina Coatings: Microstructure, Nanoindentation and Wear," *J. Therm. Spray Technol.* Vol. 25, No. 8 (2016) pp. 1700–1710.

[9] Oliver, W.C., Pharr, G.M., "An improved technique for determining hardness and elastic modulus using load and displacement sensing indentation experiments," *J. Mater. Res.* Vol 7, No. 6 (1992) pp. 1564–1583.

[10] Fischer-Cripps, A.C., *Nanoindentation*, Springer Science + Media LLC (New York, 2002) pp. 49.

[11] Shackelford, J. F. and Alexander, W., *CRC Materials Science and Engineering Handbook*. 3rd ed., CRC Press, (New York, 2001), pp. 823-824.

[12] Santisteban, J.R., Daymond, M.R., James, J.A., Edwards, L., "ENGIN-X: A third-generation neutron strain scanner," *J. Appl. Crystallogr.* Vol. 39, No. 6 (2006) pp. 812–825.

[13] Withers, P.J., Johnson, M.W., Wright, J.S., "Neutron strain scanning using a radially collimated diffracted beam," *Phys. B Condens. Matter.* Vol. 292, No. 3-4 (2000) pp. 273–285.

[14] Amada, S., Hirose, T., "Influence of grit blasting pre-treatment on the adhesion strength of plasma sprayed coatings: fractal analysis of roughness," *Surf. Coatings Technol.* Vol. 102, No. 1-2 (1998) pp. 132–137.

[15] Ganvir, A., Curry, N., Markocsan, N., Nylén, P., Toma, F.L., "Comparative study of suspension plasma sprayed and suspension high velocity oxy-fuel sprayed YSZ thermal barrier coatings," *Surf. Coatings Technol.* Vol. 268, No. 268 (2015) pp. 70–76.

[16] Aubignat, E., Planche, M.P., Allimant, A., Billières, D., Girardot, L., Bailly, Y., Montavon, G., "Effect of suspension characteristics on in-flight particle properties and coating microstructures achieved by suspension plasma spray," *J. Phys. Conf. Ser.* Vol. 550, No. 1 (2014) pp. 12019.

[17] McPherson. R, "On the formation of Thermally Sprayed Alumina Coatings," *Journal of Mat. Sci.,* Vol. 15, No 12 (1980), pp 3141-3140.

[18] Ahmed, R., Faisal, N.H., Paradowska, A.M., Fitzpatrick, M.E., "Residual strain and fracture response of Al 2O 3 coatings deposited via APS and HVOF techniques," *J. Therm. Spray Technol.* Vol. 21, No. 1 (2012) pp. 23–40.

[19] Prevéy, P.S., *X-ray diffraction residual stress techniques,* Met. Handbook. 10. Met. Park American Society for Metals (1986) pp. 380–392.

[20] Heimann, R.B., "Thermal spraying of silicon nitride coatings using highly accelerated precursor powder particles," *Surf. Coatings Technol.* Vol. 205, No. 4 (2010) pp. 943–948.

[21] Bolelli, G., Lusvarghi, L., Varis, T., Turunen, E., Leoni, M., Scardi, P., Azanza-Ricardo, C.L., Barletta, M., "Residual stresses in HVOF-sprayed ceramic coatings," *Surf. Coatings Technol.* Vol. 202, No. 19 (2008) pp. 4810–4819.